Effect of slab and transverse beam on the FRP retrofit effectiveness for existing reinforced concrete structures under seismic loading

Daniel A. Pohoryles [a], Jose Melo [b], Tiziana Rossetto [c], Humberto Varum [d] and Dina D'Ayala [e].

[a] Scientific Project Officer, European Commission, Joint Research Centre, Ispra 21027, Italy; formerly, Research Associate, Dept. of Civil, Environmental and Geomatic Engineering, EPICentre, Univ. College London, Chadwick Bldg., Gower St., London WC1E 6BT, UK (corresponding author). Email: daniel.pohoryles@ec.europa.eu

[b] Postdoctoral Fellow, Laboratory for Earthquake and Structural Engineering (CONSTRUCT-LESE), Faculty of Engineering, Dept. of Civil Engineering, Univ. of Porto, Porto 4200-465, Portugal; formerly, Research Associate, Dept. of Civil, Environmental and Geomatic Engineering, EPICentre, Univ. College London, Chadwick Bldg., Gower St., London WC1E 6BT, UK. Email: josemelo@fe.up.pt

[c] Professor, Dept. of Civil, Environmental and Geomatic Engineering, EPICentre, Univ. College London, Chadwick Bldg., Gower St., London WC1E 6BT, UK. Email: t.rossetto@ucl.ac.uk

[d] Professor, Laboratory for Earthquake and Structural Engineering (CONSTRUCT-LESE), Faculty of Engineering, Dept. of Civil Engineering, Univ. of Porto, Porto 4200-465, Portugal. Email: hvarum@fe.up.pt

[e] Professor, Dept. of Civil, Environmental and Geomatic Engineering, EPICentre, Univ. College London, Chadwick Bldg., Gower St., London WC1E 6BT, UK. Email: d.dayala@ucl.ac.uk

ABSTRACT

The seismic behaviour of reinforced concrete (RC) structures is critically influenced by the complex mechanical interactions at beam-column joints. To ensure the desired hierarchy of failure is achieved when retrofitting existing structures, numerical and experimental assessments need to represent realistic structures. A review of published literature indicates that most experimental work on the seismic behaviour pre-1970's RC beam-column connections considers sub-assemblies without slabs or transverse beams, which are unrepresentative of reality. To evaluate the effect of these elements on the failure mechanism, retrofit need and retrofit effectiveness, experiments on four full-scale beam-column joints are carried out. Two specimens with and without slab and transverse beams, are tested in their as-built and FRP strengthened configurations. As expected, the experimental results demonstrate that the progression of damage and failure mechanisms differ significantly when slabs and transverse beams are present, confirming previous numerical and experimental evidence on the strong contribution of these elements on the overall joint behaviour. Moreover, a significantly higher retrofit effectiveness is observed for the specimen without slab and transverse beam. This implies that experiments on retrofitted joints without slab and transverse beam can lead to a focus on joint shear strengthening alone as they inadequately represent the hierarchy of strengths of the framing members. They can also lead to an overestimation of retrofit effectiveness. These observations have implications when considering common simplifying assumptions made in the numerical modelling of RC moment resisting frames when assessing their seismic performance.

KEYWORDS: seismic retrofit; fibre-reinforced polymers; beam-column joints; RC slabs.

1. INTRODUCTION

Observation of soft-storey failures of reinforced concrete (RC) moment resisting frames (MRF) in recent seismic events can often be related to the inadequate seismic detailing of pre-1970's structures. The global failure of the structure due to an inadequate hierarchy of strengths around the beam-column connections, for instance leads to the formation of weak-column/strong-beam mechanisms [1]. To prevent future losses, efficient strengthening strategies are required that both delay the occurrence of damage and promote a beam-hinging mechanism when damage occurs. This can be achieved, for instance, through traditional RC-jacketing of structural elements, but also by means of composite materials such as fibre-reinforced polymer (FRP) or textile-reinforced mortars [2,3]. To achieve an effective retrofit, it is important to determine the deficiencies of existing structures in need for strengthening, which strongly depends on understanding the complex mechanical interactions within and around beam-column connections.

Under seismic loading, transverse beams and slabs, which are typically present in RC MRF buildings worldwide, can significantly contribute to the resistance mechanism of beam-column connections and alter the hierarchy of strengths between the framing members. This is recognised in design guidelines for modern structures, such as Eurocode 8 – Part 1 [4], which typically account for this effect by including an effective width of slab in the analysis of the beams. However, only limited experimental studies have assessed as-built RC joints that include slabs and transverse beams, and these have shown a significant effect of these elements on the behaviour of the specimens. Existing studies, however, either use scaled-down specimens [5], represent corner joints [6] or are seismically designed containing significant joint reinforcement [7]. These studies showed that RC slabs severely affect the failure mechanism increasing the beam moment capacity, worsening the weak-column/strong-beam hierarchy of strength in non-seismically designed structures. Transverse beams, in turn, also influence the failure mechanism, by increasing the confinement of the joint. The important effect of slab and transverse beams has also been investigated numerically in an earlier finite element study by the authors [8], which showed a different failure mechanism and different lateral capacities for the specimens without slab and without slab and transverse beams.

When assessing a structure without considering these elements, a designer may come to the wrong conclusion in terms of the needs for strengthening of a structure. Moreover, ignoring these elements when experimentally evaluating a retrofit scheme additionally renders the existing structure more accessible. This does not give a realistic picture of the practical challenges and feasibility of the schemes, including need for and placement of anchors. A previous review of published literature has shown that most experimental studies on the seismic behaviour of FRP-retrofitted pre-1970's RC joints do not consider slabs or transverse beams in their experimental set-ups (82%), which are partially unrepresentative of reality [2]. The focus on simpler, cross-shaped, beam-column joints has led to a majority of studies looking at joint panel shear strengthening interventions alone, without considering other issues of importance with respect to achieving a seismic behaviour following a capacity-design philosophy. For instance, post-earthquake reconnaissance studies indicate that single-storey weak-column failures are most commonly observed in deficient RC buildings [5,9], but only 11% of previous experimental studies on beam-column joint sub-assemblies considered a weak-column/strong-beam deficiency in the FRP-retrofit design [2].

Previous experimental studies have further shown that the consideration of the presence of slabs can be crucial for the assessment of retrofit effectiveness. For example, a beam-hinging mechanism may not be achieved with FRP strengthening of the columns alone, but additionally requires selective-weakening of the RC slab when considering an inadequately designed beam-column joint sub-assembly with slabs [10,11]. Not including the slab in the test specimens, or only increasing the top-reinforcement of the beams to represent the effect of the slab, would not have highlighted this issue of significant stiffness increase of the beams, which prevents rotation in the beams to change the damage mechanism. Changes in failure mechanisms, and hence differences in retrofit priorities, may also lead to a reduction in retrofit effectiveness in terms of base-shear capacity and ductility, as highlighted in the authors' previous analysis [2]. It was observed that the retrofit of specimens without slab and transverse beam are significantly more effective in increasing strength (+44%) than for more realistic geometries (+27%), indicating an effect of these elements for a wide range of different specimens and retrofit designs. This is even more critical in terms of displacement ductility, with an average increase of 63% for cross-shaped specimens, compared to only 38% for specimens with slab and transverse beams. Clearly, these differences on a large set of experiments must be taken with care. The reduced retrofit effectiveness for specimens with slab or transverse beams may be related to differences in strengthening configurations, due the reduced accessibility of the joint, but also beams and columns, but also to changes in damage and failure mechanisms and differences in retrofit design priorities. To truly assess the effect of slab and transverse beams on the retrofit effectiveness, it is hence important to test this hypothesis on specific set-ups, using the same (or similar) retrofit on a specimen with and without slab and transverse beams. Akguzel and Pampanin [12] tested a GFRP retrofit scheme on a corner joint with and without slab and found retrofit effectiveness to be reduced for the specimen with slab. Crucially, the failure mechanism of the retrofitted specimens was also observed to be different. Antonopoulos and Triantafillou [13] compared the performance of a CFRP retrofit on an exterior joint with and without transverse beam. Again, the strength enhancement for the specimen with transverse beam was significantly lower (up to −78%).

This impact of slabs and transverse beams on the retrofit priorities and effectiveness is of particular importance considering that several design guidance documents base their recommendations on experimental evidence from specimens that did not include slabs and transverse beams. For instance, The fib Bulletin 35 [14] dedicates a section on 'Seismic retrofitting of RC beam-column joints using FRP', looking only at experimental work on 2-D joints [15,16], but indicating the importance of analytically accounting for the 'confining effect of transverse beams and slab contribution'. The latest fib Bulletin 90 [17] addresses the retrofit of joints in section 8.7, considering experimental work carried out on joints without slabs [13,18–20]. However, a 'note of caution' is made regarding the 'geometric complexity of actual 3-D frame connections which also include slabs'. The importance of slabs is recognised, but no actual practical solution is offered on how to 'achieve uniform and effective confinement' of the joint, referring instead to the 'inventiveness and versatility of the engineer'. Suggested lay-outs for retrofit application only consider joint panels that are fully accessible for full FRP-confinement. In the US, the ACI 440.2R-17 [21] chapter 13 on seismic strengthening refers to experimental evidence from exterior and interior joint tests without slabs is taken [22,23], but also recognises the work by Engindeniz et al. [24] who tested corner joints with slabs.

The design of retrofit solutions for RC structures may hence be based on experimental efforts that do not entirely reflect reality, as well as analyses of two-dimensional frames, which neglect the transverse beam and slab effects on confinement of the joint and beam capacity. It is postulated that the response of beam-column connections, may be inadequately represented when omitting slab and transverse beams, leading to easier retrofit applications and changes in failure mechanism and retrofit needs. Based on limited experimental evidence, this could lead to higher expected retrofit effectiveness. Recently, the authors proposed and tested a capacity-designed FRP-retrofit methodology, considering not only joint shear strengthening with the presence of transverse beams, but also flexural strengthening of the columns combined with selective weakening of the slabs to achieve a beam-hinging mechanism [25]. The objective of this study was to understand the effect of specimen geometry on the retrofit effectiveness from a holistic perspective, looking at changes in overall failure mechanism and strength increase, which do not relate to the shear capacity of the joint panel alone, but also the framing members. To achieve this, an experimental comparison for this retrofit layout was carried out on full-scale pre-1970's interior beam-column joints with and without slab and transverse beams are conducted in this study. The effect of slab and transverse beams is assessed for the control specimens and their retrofitted counterparts. The evaluation considers the respective failure mechanisms, as well as various performance diagnostics, including strength of the sub-assembly, displacement ductility, energy dissipation and post-peak softening.

2. EXPERIMENTAL PROGRAM

2.1. SPECIMEN DETAILS AND MATERIAL PROPERTIES

Four specimens were tested in this study, summarised in Table 1, consisting of two control specimens, one with slab and transverse beams (C1), and one cross-shaped specimen without slab and transverse beams (C-noSLT), as well as their respective retrofitted versions, C1-RT-B-sw and C-noSLT-RT-B. The label 'sw' refers to selective weakening, where cuts in the slab have been made to reduce its contribution to the beam hogging capacity. The test specimens are designed to represent real-scale interior beam-column joints in a four-storey RC MRF structure, as described in [25], in which the results of C1 and C1-RT-B-sw were initially reported. The detailing of the specimens aims to replicate common deficiencies of pre-1970's residential buildings in Southern Europe (e.g. weak-column/strong-beam mechanism and inadequate joint shear capacity) and is based on the design guidance given in the 1967 REBA [26] Portuguese RC code. A normalised base shear factor for lateral load of the 0.05 of building weight (273 kN) is used for the design for seismic zone C.

The geometry and reinforcement detailing of the specimens are shown in Fig. 1. Note that the columns with a length of 1.50 m represent the half-storey above and below the joint. Similarly, the main beam has a length representative of a half-span in the designed building. For specimens C1 and

C1-RT-B-sw, a 1.95 m wide and 150 mm deep slab, as well as a 0.825 m long transverse beams are included. The transverse beams have the same cross-sectional dimensions and reinforcement detailing as the main beams.

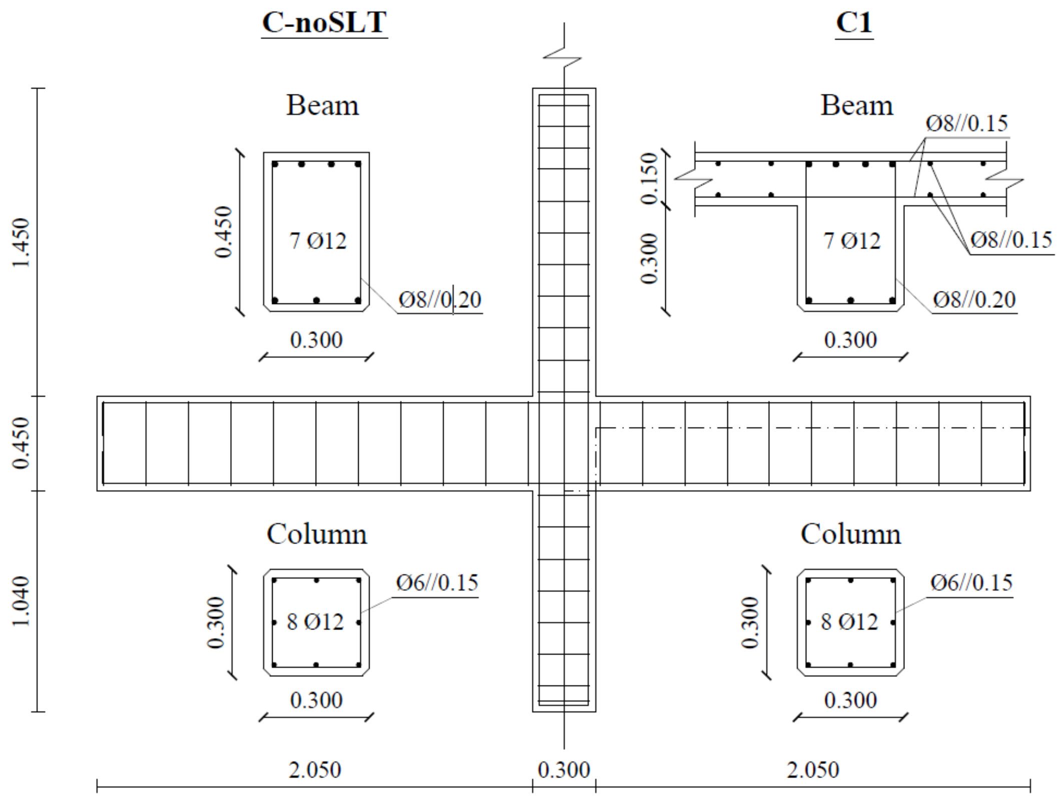

Fig. 1. Reinforcement detailing of the specimens - dimensions in m, bar size in mm.

The concrete mean compressive strength (f_{cm}) for each specimen is obtained from crushing six cylinder samples (Ø150 x 300 mm) and is summarised in Table 1. The ultimate strength ($f_{u,FRP}$) and strain ($\varepsilon_{u,FRP}$), as well as elastic modulus (E_f) and thickness (t_f) are given in Table 2. The CFRP is S&P C-240 sheet and its tensile strength is evaluated using the ISO/DIS 10406-2:2013 characterisation tests. The results of steel tensile tests are reported and Table 3, showing the yield stress (f_y) and strain (ε_y), as well as the ultimate strength (f_u) and strain (ε_u) for the three bar sizes.

Table 1. Summary of test specimens, including concrete strength and flexural strength ratios.

Specimen	Description	f_{cm} (MPa)	$\Sigma M_c / \Sigma M_b$
C1	Control specimen with slab and transverse beam	23.4	0.75
C-noSLT	Cruciform control specimen without slab and transverse beam	29.6	1.25
C1-RT-B-sw	Retrofitted specimen with slab and transverse beam	19.3	1.3

C-noSLT-RT-B	Cruciform retrofitted specimen without slab and transverse beam	29.6	1.37

Table 2. CFRP material properties.

Material	t_f (mm)	$f_{u,FRP}$ (MPa)	$\varepsilon_{u,FRP}$ (%)	E_f (GPa)
S&P C-240	0.223	3300	1.7	194.1

Table 3. Steel reinforcement mean material properties (yield stress - f_y and ultimate stress - f_u).

Bar diameter	Φ12	Φ8	Φ12
f_y (MPa)	450	540	538
ε_y (%)	0.0022	0.0025	0.0026
f_u (MPa)	570	570	645
ε_u (%)	21	18.5	16

2.2. Assessment of seismic design deficiencies of the control specimen

Overall, a brittle failure mechanism is expected for the control specimens due to their non-compliance with capacity design principles. The control specimens were designed with an inappropriate hierarchy of strengths, i.e. a lower flexural capacity of the columns than the beams (weak-column/strong-beam mechanism) and a low shear capacity of the joint. The former was evaluated by calculating the ratio of the flexural capacities of the columns and beams (ΣM_c / ΣM_b) from a capacity design perspective. The ratios, given in Table 1, were calculated from the relative design moment capacities according to Eurocode 2 [27] and Eurocode 8 – Part 1[4]. For the beam hogging moments, according to EC8 cl. 5.4.3.1.1(2), an effective width of the slab was considered, corresponding to four times the thickness of the slab, h_f. Consequently, the flexural strength ratio of specimen C1 was determined to be significantly lower (ΣM_c / ΣM_b = 0.75) than the recommended capacity design ratio of 1.3 (0.75 for specimen C1).

To consider selective weakening, the effective width was reduced to the part of the slab that was not cut, which corresponds to a length of 1.5 · h_f (450 mm). Note that selective weakening alone would lead to an increased value of ΣM_c / ΣM_b = 0.94 for C1, but still inferior to the desired value. Finally, when not considering the slab, the ratio of the moment capacities of the columns to the beams in C-noSLT is significantly higher (1.25), albeit still below the recommended design value. This would lead to a different retrofit priority for this specimen, typical of the interior joints tested in the literature where the contribution of the slab is not commonly considered.

Further inadequacies of the control specimen lie in the lack of shear reinforcement in the joint, as well as a lack of confinement in the columns due to inadequate transverse reinforcement spacing. The joint shear demand and joint shear capacity verification for retrofitting in Eurocode 8 – Part 3 [28] was performed according to Eurocode 8 – Part 1, sections 5.5.2.3 and 5.5.3.3. The shear capacity of the control specimen C1 ($V_{jh,max}$ = 596.2 kN), calculated to eq. 5.33 of Eurocode 8 – Part 1 was found to be sufficient for the capacity design shear demand (V_{jhd} = 564.1 kN), i.e. taking into account the most adverse conditions under seismic actions. Note that this situation however changes for the retrofitted specimen, with an increased joint shear demand, as explained in the next section.

2.3. FRP RETROFIT DESIGN AND APPLICATION

The FRP retrofit scheme RT-B-sw in this study considers the practical limitations in a specimen with slab and transverse beams explicitly (Fig. 2). This retrofit scheme is presented in more detail in Fig. 3 and in [25], where it is seen to provide an optimum retrofit to achieve a beam-sway mechanism with plastic hinge formation one beam-depth away from the joint interface, with high strength and ductility, and hence a similar performance to a structure designed to modern guidelines.

Fig. 2. Retrofit applied to a specimen with slab and transverse beams.

To determine the required amount of CFRP in the respective members and calculate the capacities of the retrofitted members, as well as appropriate development lengths for the sheets, an adaptation of the CNR-DT-200.R1/2013 [29] guidelines was implemented, details of which can be found elsewhere [30]. In brief, the retrofit, which was designed for specimen C1, is carried out with three main aims: (1) to address the weak-column/strong-beam hierarchy of strengths; (2) to carry out a plastic hinge relocation in the beams; and (3) to protect the joint from an increased joint shear demand and yield penetration.

(1) As the flexural strength ratio of columns to beams (ΣM_c / ΣM_b) was found to be lower than the recommended capacity design ratio of 1.3, a retrofit of the columns was determined to be necessary. Simply improving the confinement of the columns by FRP-wrapping was not found to be sufficient to achieve an adequate flexural strength ratio. Instead, a novel flexural strengthening method was developed, using FRP-strands (shown in red on the columns in Fig. 3), which were passed through plastic tubes at the corners of the column to achieve continuous strengthening between bottom and superior column. The strands, made from six layers of 250 mm wide vertical FRP sheets, were mechanically anchored at their ends using steel anchors. Details of the retrofit scheme with the strands were previously presented in [25]. To anchor the flexural strengthening, but also to protect the columns from shear failure due to the increased shear demand following retrofitting, three layers horizontal FRP wraps were also applied for confinement and shear strengthening of the columns (not shown in Fig. 3). These layers of horizontal wrapping also protect the columns from bar-buckling failure.

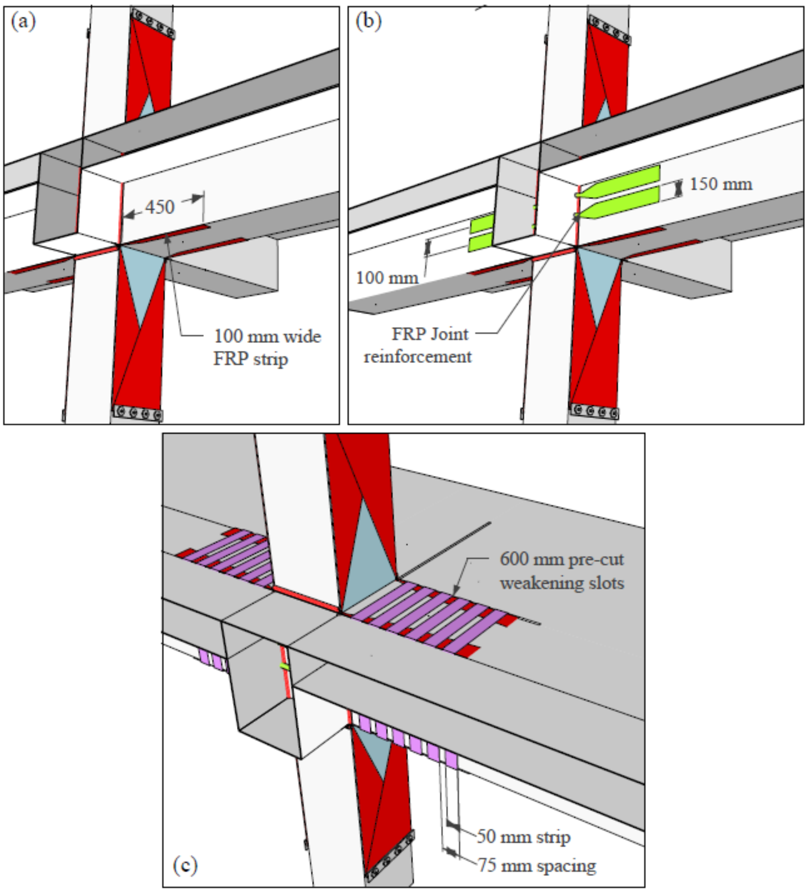

Fig. 3. Dimensions of retrofit RT-B-sw: (a) beam strands; (b) joint strands; (c) beam transverse strips.

Flexural strengthening of the columns alone was determined to be insufficient to ultimately prevent a column-sway mechanism in previous experimental research by the same authors [10]. This was due to the strong contribution of the RC slab to the beam flexural capacity and stiffness of the beams. Selective weakening of the slab was hence found to be required to ensure formation of a beam-sway mechanism. Weakening cuts through the slab reinforcement along a length of two column depths from the columns face (600 mm) were performed as part of the retrofit.

(2) With damage being transferred from the column to the beams, avoiding yield penetration into the joint core was deemed crucial, as yield would occur at the beam/joint interface. To avoid this and ensure joint integrity, FRP strengthening was hence applied to the beams near the beam/joint interface to relocate plastic hinge formation by one beam-depth (450 mm) from the joint interface. This length was determined adequate in the analysis of previous experimental work [31]. To achieve plastic hinge relocation, two 100 mm wide FRP strands (shown in red on the beams in Fig. 3) were applied at the top and bottom faces of the beams, along a length of 450 mm of the beam and through the joint area to achieve continuity and an adequate development length. End-anchorage of the FRP was provided by means of steel plates. Due to the increase in flexural demand of the beams, the shear demand also increases, hence beam shear-strengthening consisting of 50 mm wide strips spaced at 75 mm, was applied as full wraps through holes drilled in the slabs (shown in purple on the beams in Fig. 3).

(3) While interior joints with four framing beams are generally considered to be less shear critical, after retrofitting the framing members, (and the associated increase in the strength of the beams and columns), an increase in joint shear demand to 598.3 kN is obtained. This value exceeds the design joint shear capacity calculated to eq. 5.33 of Eurocode 8 – Part 1, and joint shear strengthening was required. This is confirmed by previous experiments on the same specimen strengthened in the columns only, without joint shear strengthening, which displayed shear-damage to the joint panel [10,30]. To achieve joint shear strengthening, horizontal FRP strands were placed through holes drilled at the transverse beam/joint interface (shown in green on the beams in Fig. 3). These strands consisted of two rolled-up 150 mm wide strips, splayed out and extended for 300 mm onto the beam flanges and anchored using bolted steel plates to avoid end-debonding. The increase joint shear strength,

calculated according to cl. 4.19 of the CNR guidelines, was 64.0 kN, i.e. exceeding the demand.

The same retrofit scheme was adapted for the case of a specimen without slab and transverse beam (retrofit RT-B), as shown in Fig. 4. Note that the retrofit was not designed for this specimen, but the same amount of FRP in all members is kept equal in both retrofit schemes to evaluate the relative effectiveness of retrofit schemes for specimens with and without slabs and transverse beams. The, actual application was however slightly different due to the differences in geometry. For instance, the joint shear strengthening is applied directly on the joint face in form of two strips, instead of the application of rolled-up strands passed through holes in the transverse beam, as for the specimen with slab and transverse beams. This may have an unquantifiable effect on the strengthening effectiveness, it is however not possible to achieve exactly the same retrofit application in the absence of the transverse beams. For the beams, the transverse reinforcement is also more easily applied, as no cuts in the slab are required to achieve full wrapping.

Fig. 4. Retrofit applied to a specimen without slab and transverse beams.

2.4. Test set-up and loading

The four specimens are tested using a quasi-static cyclic drift (Δ) protocol applied with a hydraulic actuator at the top of the superior column, 1.5 m from the centre of the joint core, using the set-up shown in Fig. 5. Each drift cycle is repeated three times and drift values increase from ±0.1, 0.2, 0.3, and then 0.5 up to 6.0 % in 0.5 %. The rate of displacement application hence ranges from 0.1 mm/s in the first cycles up to 1.5 mm/s in the last cycles. A constant axial load (N1) of 425 kN is applied for all specimens through external pre-stress rods, pin-jointed at the top of the superior column and the bottom support of the inferior column. An additional axial load (N2) of 25 kN is applied at the inferior column to induce moments in the beams simulating gravity loading. The value of N1 was calculated for a second storey column in a typical residential four-storey RC frame in Europe. Further details on the instrumentation and loading set-up can be found in the associated *MethodsX* article and in [25].

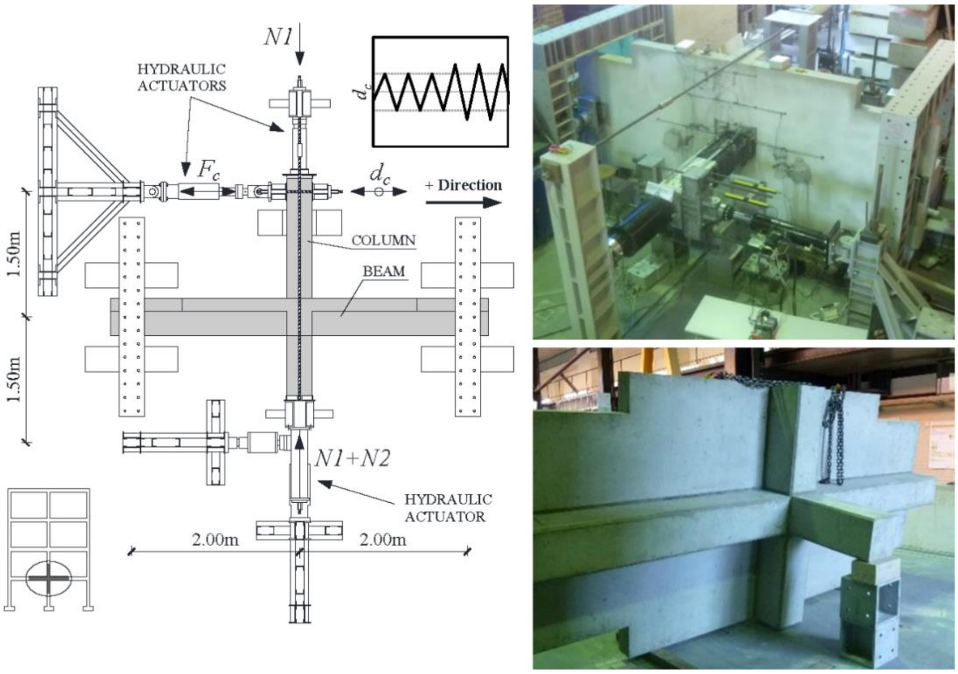

Fig. 5. Test set-up with prototype structure and sample loading protocol.

3. EXPERIMENTAL RESULTS

The main experimental results for the four full-scale tests are presented in this section. The general results are presented first, followed by a detailed description of the damage mechanism and observed phenomena for the control and retrofitted specimens. In section 4, an in-depth analysis in-depth analysis of the results, including multiple criteria, such as the energy dissipation, ductility, initial stiffness, and softening behaviour.

For all specimens, the global lateral force–displacement behaviour presented in Fig. 6 in the form of hysteresis curves. The first occurrence of cracking, spalling, buckling and yielding are indicated on the force-displacement plots to aid assessment of the specimens. In Table 4, a summary of the main experimental results is shown, including the maximum force (F_{max}), the location of observed failure, the cumulative energy dissipation (E_d) and the initial peak-to-peak lateral stiffness (K_i). In the table, the ultimate displacement ductility, $\mu_{\Delta u}$, is defined as the ratio of ultimate drift, Δ_u, reached when a strength reduction of 20% from F_{max} is observed [32], and yield drift, Δ_y, at which the first strain gauge reading exceeds the steel yield strain (0.2%). The post-peak softening (*S*), defined as the slope between F_{max} and F_u, the force at ultimate drift, Δ_u, is also presented in Table 4 as an indirect measure of residual strength. The reader is referred to the associated *MethodsX* article for further details on the calculation of these parameters.

Table 4. Summary of experimental results.

Specimen	F_{max} [1] (kN)	Failure	Δ_y (%)	$\mu_{\Delta u}$ Δ_u / Δ_y	E_d (kNm)	S (kN/mm)	K_i (kN/mm)
C1	63.1	Sup. column	0.65	3.6	32.1	-0.49	6.6
C1-RT-B-sw	86.9 (+38%)	Beams, Column	0.95 (+55.7%)	6.9 (+89.6%)	111.6 (+247.8%)	-0.19 (-61.8%)	5.7 (-14.5%)
C-noSLT	45.2 (-28%)	Joint	0.67 (+10.2%)	5.2 (+44.4%)	31.8 (-0.8%)	-0.15 (-70.2%)	4.8 (-27%)
C-noSLT-RT-B	67.8 (+50.2%)	Beams	1.06 (+57.3%)	2.8 (-45.9%)	19.2 (-39.6%)	-0.83 (+464.6%)	3.8 (-20.4%)

[1] Note: % difference in brackets compared to C1, apart from C-noSLT-RT-B, for which C-noSLT is the control specimen

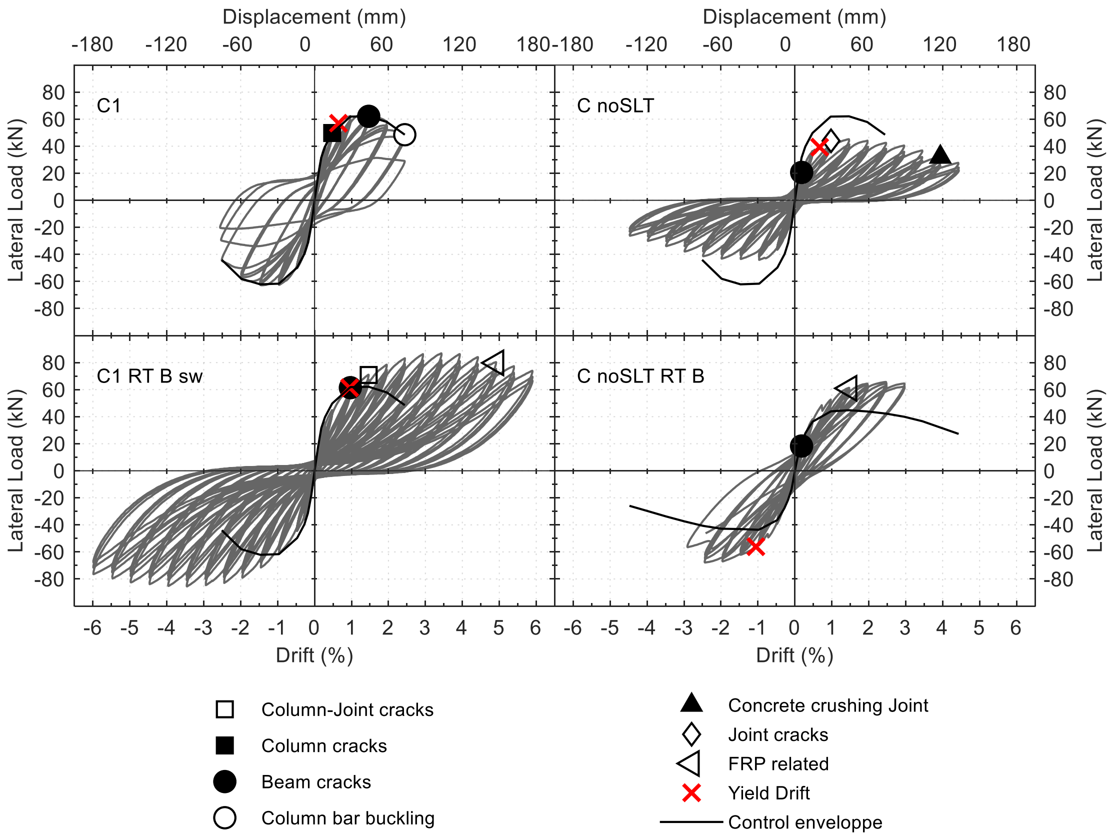

Fig. 6. Lateral load versus drift hysteresis curves with damage for all specimens.

3.1. Behaviour of control specimens

For the control specimen with slab and transverse beam, C1, as expected for a pre-1970's structure, an undesirable single-storey column failure mechanism is observed. The failure is characterised by large rotation of the superior column and localised plastic hinge formation near the joint. The sequence of observed damage is presented in Fig. 6 and shows that initial cracks already form in the superior column during the 0.5% drift cycles, with yielding of the column bars following at 0.65% drift. A relatively low peak lateral force of 63.1 kN is recorded at 1.3% drift. After plastic hinge formation, due to the inadequate spacing of lateral reinforcement, and hence lack of confinement, concrete crushing and buckling of the reinforcing bars is observed at the base of the superior column (Fig. 7 a).

(a) (b)

Fig. 7. Final damage state in C1: (a) superior column; (b) beam underside.

No significant damage is instead observed in the rest of the structure, with only minor cracks and no yielding of beams bars seen due to limited rotation of the beams. It is worth noting that two cracks along the entire width of the slab can be observed perpendicular to the loading direction in Fig. 7 (b), which indicates the slab contribution to the behaviour of the specimen. The observed failure is characterised by a low cumulative energy dissipation (32.1 kNm) and significant post-peak softening, with a drastic reduction in load bearing capacity (up to 2.3% drift), leading to a displacement ductility of 3.6 (Table 4).

For the cruciform control specimen, C-noSLT, different damage mechanisms are observed as compared to C1. Joint shear failure dominates the behaviour, and unlike C1, no significant cracks are observed along the column. Instead, lack of confinement from the transverse beams and reduced beam capacity due to the missing slab cause damage concentrated in the joint panel, as well as cracking along the length of the beam, as shown in Fig. 8 (a) and (b), respectively. This joint-dominated damage mechanism is highlighted by a large level of joint shear distortion shown in Fig. 9.

Significant joint shear strength degradation is observed for specimen C-noSLT up to the peak joint shear distortion of 0.065 rad. The maximum sustained tensile stress in the joint is 0.39 √fc in specimen C-noSLT.

(a) (b)

Fig. 8. Final damage state in C-noSLT; (a) joint, (b) beam.

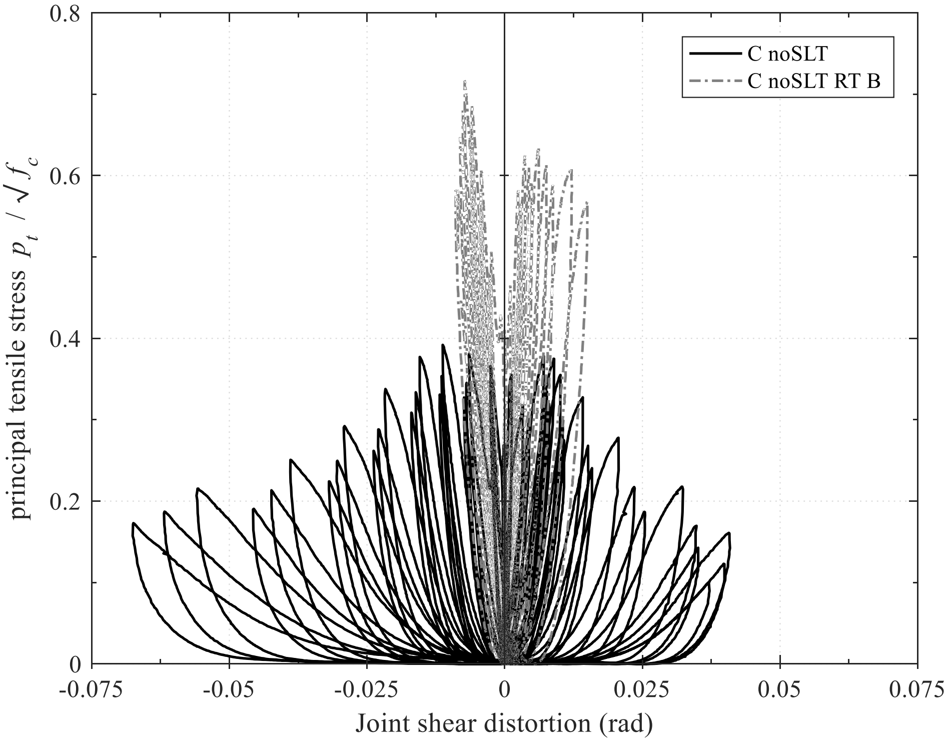

Fig. 9. Principal tensile stress (normalised by concrete strength) against joint shear distortion for C-noSLT-RT B compared to control specimen C-noSLT.

The damage progression seen in the hysteretic curve (Fig. 6) also highlights that beams and joint dominate the specimen's behaviour. Initially, thin cracks are observed in the beams at very low drift cycles (0.2%), It is worth noting that, as a consequence of simulating the effect of gravity loading on the beams in the experimental set-up, larger hogging than sagging moments are developed in the beams near the joint. In the absence of the slab, yield hence initialises in the top beam bars at 0.67% drift near the interface with the joint.

During the 1.0% drift cycle, cracks in the joint appear. The maximum lateral load of 45.16 kN is reached at 1.46% drift. The post peak behaviour is dominated by damage concentration in the joint. The results in Table 4 show that despite joint failure, softening is less accentuated than for specimen C1 (-70.2%) and a large displacement ductility of 5.2 is reached. As for C1, this is partly due to a low yield drift. After reaching the ultimate state (20% capacity drop) at 3.5% drift, concrete crushing in the corners of the joint is observed (4.0% drift), followed by spalling in the joint panel (4.5%).

3.2. Behaviour of retrofitted specimens

The retrofitted specimen with slab and transverse beam, C1-RT-B-sw, presents a very ductile behaviour and a significant increase in lateral load capacity (+37.7%) compared to its control specimen. As for C1, a large crack at the interface between the slab and the upper column is observed, however from Fig. 10 (b) it can be seen that the rotation of the beams is significantly increased. The damage and plastic hinge formation in the beam occurs away from the joint, as anticipated by the design. Compared to the control specimen, damage is delayed with onset of yielding and cracking in the beams observed at 1% drift. As shown in Fig. 10 (b), cracks in the beam bottom face are spread along its length, with cracks appearing in the envisaged plastic hinge zone (one beam depth away from the joint interface) at 1.5% drift.

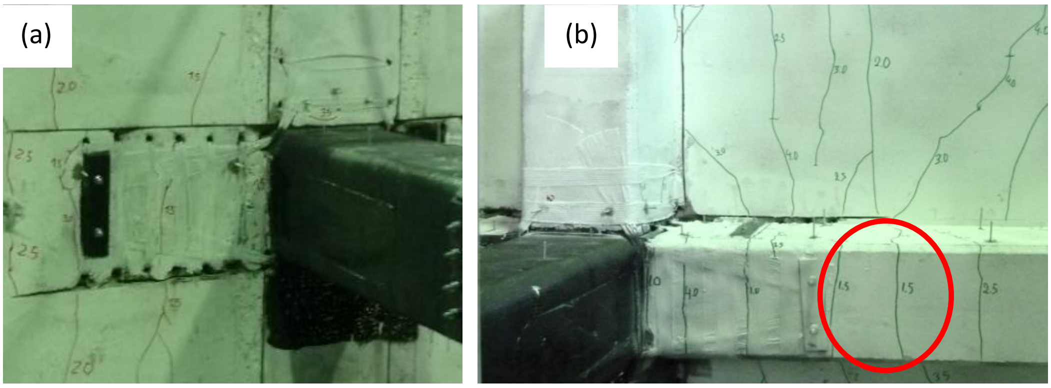

Fig. 10. Final damage state in C1-RT-B-sw; (a) column and slab, (b) beam underside. Envisaged plastic hinge zone circled in red.

Despite the presence of cuts in the slab at its interface with the beams, cracks are seen to extend fully across the width of the slab from the 2.0% drift cycles onwards. Multiple parallel cracks perpendicular to the main beam axis are observed first, followed by diagonal cracks in the slab bottom face originating from the end of the selective weakening cuts (3.0% drift). Ultimate failure is reached after partial rupture of the FRP strand along the main beam (indicated in Fig. 3 a) is observed. Visual observation during the test however indicates that this rupture is not caused by excessive tensile strain, but as a consequence of a shearing mechanism due to contact with the transverse beam FRP strand. Despite crack opening at the upper column base, the maximum recorded strain in the vertical FRP strands remains significantly lower than the debonding or rupture strain (0.08%).

Joint integrity is preserved in the specimen up large levels of drift. This is due to activation of the FRP strands passed through the joint, which is confirmed by strain readings up to 0.12%. No damage in the joint core is observed after testing when the transverse beams are removed. It is highlighted that in a specimen previously tested with a similar strengthening scheme, but without joint core strengthening, the joint did suffer damage [33]. This confirms the importance of the joint strengthening strands when a retrofit scheme leads to higher load and displacement demand. Overall, the specimen behaves according to the envisaged hierarchy of strengths from the retrofit design leading to a strongly improved softening behaviour (-61.8% compared to C1), and hence a more ductile (+89.6%) and dissipative failure mechanism (+247.8%).

With the absence of slab and transverse beams for the retrofitted cruciform specimen C-noSLT-RT-B, damage in the beams and joint is more pronounced, as shown in Fig. 11 (a) and (b), respectively. No damage or FRP debonding are observed in the columns. In terms of joint shear damage, the behaviour of C-noSLT-RT-B is significantly improved compared to C-noSLT. While diagonal cracks below the joint-shear strengthening were observed from 1.0% drift onwards (which led to partial FRP debonding in the joint panel at 1.5% drift), the joint retains its integrity throughout testing. This can be attributed to significant activation of the two FRP strips in the joint, for which a maximum strain of 0.46% is measured. This is nearly four times the value recorded for C1-RT-B-sw (0.12%). The improved joint shear behaviour is apparent in the plot of principal stress against joint shear distortion in Fig. 9. While strong joint shear strength degradation with increased distortion is observed for the control specimen C-noSLT, the joint displays an elastic behaviour for C-noSLT-RT-B with significantly reduced distortion (-75%). The FRP strips clearly strengthen the joint with tensile stress reaching 0.72 $\sqrt{fc}$; an increase of 84% compared to specimen C-noSLT.

(a) (b)

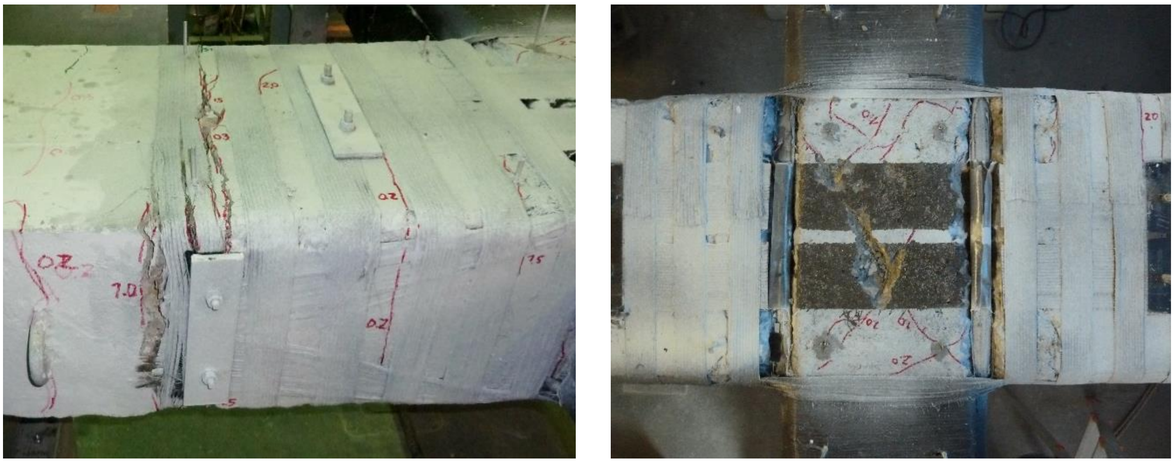

Fig. 11. Specimen C-noSLT-RT-B: (a) large crack opening at beam; (b) diagonal cracks in the joint panel after removal of FRP.

As a consequence of joint shear strengthening, a significant increase in lateral load capacity (+50.2%) is obtained for C-noSLT-RT-B compared to its control specimen C-noSLT as shown Table 4. Due to the plastic hinge relocation, large flexural crack opening in the beams at about 500 mm from the joint interface is observed from 1.0% drift onwards. This leads to loss of mechanical anchorage of the beam FRP strengthening (Fig. 11). This causes a sudden drop in capacity at -3% drift. As a result of this brittle failure, substantial softening can be observed in the hysteresis curve of Fig. 6 (+456.6% vs C-noSLT) and corresponding very low ductility of 2.8 (-45.9%) and reduced energy dissipation of 19.2 kNm (-39.6%). This could be avoided through a more distributed anchorage placement.

4. Analysis and Discussion

The experimental results of the specimens with and without slab and transverse beams show significant differences in response and damage mechanism. The effect of slab and transverse beams is clearly seen when comparing the control specimens C1 and C-noSLT and their respective failure mechanisms. Specimen C-noSLT displays a more ductile response (+44.4% vs C1), but with a much lower peak force (-28%) and a decreased energy dissipation (-0.8%). The initial stiffness of the specimen without slab is also much lower (-27%). For the control specimen without slab and transverse beam, C-noSLT, a very different damage pattern is observed, with concentration of damage in the joint region, with some cracking along the beam and very limited cracking in the columns. This is in stark contrast to the single-storey failure observed for C1. For C1 only limited rotation of the beams is observed and damage is concentrated in the column at its interface with the joint.

When identifying the contribution of individual RC members to the total energy dissipation of the specimens in Fig. 12, the consequence of reduced beam rotation in C1 with slab is clear. Nearly 80% of the total energy dissipation is dissipated by the columns, whilst only 1.5% can be attributed to the beams. For C1 a much lower curvature in the beams is recorded (- 90.2% vs C-noSLT) and the rotation of the beams is also highly asymmetric. In the case of C-noSLT, the absence of the slab means that hogging and sagging moment capacities of the beam are similar, allowing the beams and joint to rotate. This leads to 20.4% of the total energy dissipated by the beams and the majority of energy dissipated by the joint (68.1%), with the column contribution reduced to 11.5 %.

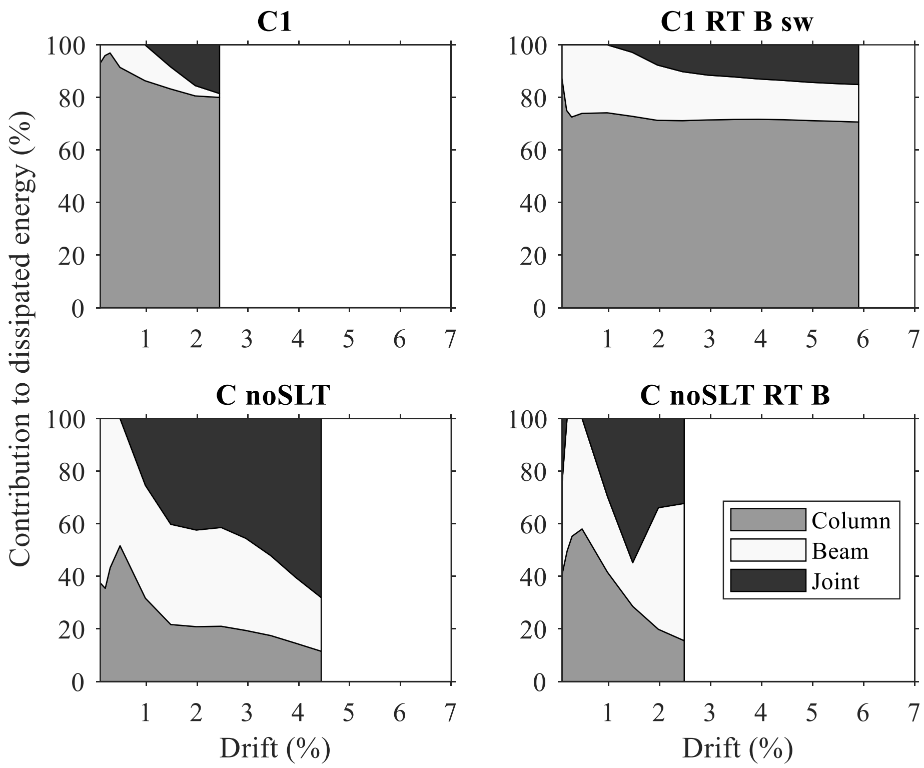

Fig. 12. Energy dissipation by individual members (Column, Beam & Slab, Joint panel) for all tested specimen.

The observation of different damage mechanisms for the control specimens with and without slabs and transverse beams in the experiments echo previous observations in a detailed finite-element analysis [8], which found differences in failure mechanism, as well as strength and ductility between C1 and C-noSLT, and are in line with limited published experimental evidence [5,7]. The latter observed that the contribution of slabs and transverse beams can be underestimated by current guidelines. This difference in failure mechanism affects the retrofit objectives significantly, as retrofit designs based on experiments conducted on cruciform interior joint specimens like C-noSLT focus on joint shear strengthening, while in reality, post-earthquake reconnaissance studies indicate that single-storey weak-column failures are more commonly observed [5,9]. In real structures with RC slabs and transverse beams, the additional hogging capacity from the slab reinforcement, as well as increased joint confinement from transverse beams, means that the failure mechanism of C-noSLT is not observed for interior joints.

The main hypothesis tested in the experiments was however linked to the observation in the literature of an overestimated effectiveness of retrofits when testing cruciform configurations compared to more realistic specimens with slab or transverse beams. The analysis of previous experimental work indicated a strength increase of 45% for cross-shaped specimens compared to 26% for FRP-retrofitted joints with slab and transverse beams [2]. For the two specimens C1-RT-B-sw and C-noSLT-RT-B tested in this study, retrofitted with the same procedure and amount of FRP, the difference in effectiveness is less pronounced, but still significant, with an increase in strength of 37.7% with slab and 50.2% without slab, respectively.

In turn, the performance of the retrofit for specimen C-noSLT-RT-B in terms of ductility and softening behaviour is observed to be reduced (Table 4). This is however associated to the loss of anchorage after significant damage to the beams. This heavy damage is a direct consequence of the retrofit increasing beam participation and rotation. For the specimen without slab, ensuring failure by a beam-sway mechanism in C-noSLT-RT-B is achieved by retrofitting the joint to eliminate joint shear failure. The different hierarchy of strengths between the respective control specimens, reduces column damage in the specimen without slab. The effectiveness of inducing beam failure is clearly observable when looking at the contribution of individual RC members to the total energy dissipation in Fig. 12. For the specimens without slab, an increase in energy dissipation due to the beams from 20.4% in C-noSLT to 52.2% in C-noSLT-RT-B is obtained, corresponding to 31.8 pp. This increase can be attributed to an increase in beam rotation combined with a reduced joint shear deformation in C-noSLT-RT-B. For the specimen with slab however, the beam participation to the total energy dissipation is only moderately increased from 1.5% in C1 to 14.4% in C1-RT-B-sw (+12.9 pp). Beam damage and rotation are observed, but the column still dominates the dissipative behaviour of the specimen, and displays substantial damage despite significant strengthening. This is a consequence of the slab resisting beam rotation despite selective weakening, which renders moving damage to the beams challenging.

Overall, the experiments conducted on specimens with slab and transverse beams is shown to have a clear effect on the behaviour of retrofitted joints. The observed damage and location of damage in specimens without slab impacts the retrofit design and effectiveness, as highlighted by the experiments presented in this study.

5. CONCLUSIONS

In this study, the importance of considering the presence of slabs and transverse beams when testing and assessing existing structures was investigated by means of four full-scale experiments on deficient RC beam-column joints. Two specimens, with and without slabs and transverse beam, were tested in their as-built and retrofitted configurations. For the as-built control specimens, load carrying capacity and failure mechanism of the specimens were observed to be significantly affected by the presence of slab and transverse beams. The contribution of the slab dictates the hierarchy of strengths, causing a single-storey column-hinging mechanism to form in specimen C1. Instead, behaviour of the specimen without slab (C-noSLT) is dominated by a joint shear failure, which was not observed in C1 due to increased joint confinement and reduced beam mobility. The latter was confirmed by a significantly lower curvature in the beams (-90.2%) for specimen C1. This stark contrast in failure mechanisms and capacities clearly affects FRP retrofit design, as a wrongly identified failure mechanism can result in focussing the strengthening intervention on the wrong target elements. This is of particular importance considering that most interior joints tested in the literature focus on joint shear-strengthening alone and may not sufficiently consider the hierarchy of strengths of the sub-assembly.

To assess the consequence of slab and transverse beams on the retrofit effectiveness, two specimens C1-RT-B-sw and C-noSLT-RT-B were retrofitted using the same procedure and same amount of FRP strengthening material. The retrofit was designed from a capacity-design perspective, looking at changing the overall failure mechanism of the joint sub-assembly to a more ductile and dissipative beam-hinging failure. To address the inadequate flexural strength ratio of columns and beams, a combined retrofit and selective slab weakening retrofit was devised and shown to effectively transfer damage to the beams, and to promote a stronger beam participation in the energy dissipation in the specimen with slab and transverse beams. Due to the increase in developed beam moments, joint shear strengthening was performed, and was shown to effectively prevent damage in the joints, which was not the case in previous efforts without joint strengthening. For the cross-shaped specimen without slab and transverse beams, the strength increase was significantly more pronounced (+50.2% vs +38%). The results from this experimental study echo observations made in a previous analysis of the experimental literature and strengthen the initial hypothesis that tests on cruciform specimens may overestimate the effectiveness of retrofit schemes. However, the retrofit scheme was shown to be less effective for the specimen without slab in terms of ductility and softening behaviour. This was related to a failure in the anchorage system following beam-hinging, indicating a need for improving this aspect of the retrofit scheme.

A more detailed analysis of the experimental results highlighted that the proportion of energy dissipation from the beams significantly increases for both retrofitted specimens, particularly for higher drift levels. Moreover, the contribution of the joint core to energy dissipation is reduced, and especially so for specimen C-noSLT-RT-B, confirming the success of the joint shear retrofit to significantly reduce observed damage in the joint panel.

Moreover, experiments on realistic specimens were shown to be important to prove the feasibility of the proposed retrofit scheme and to address practical requirements such as drilling small holes at the beams and column corners or the need for cutting through members, as well as the location of anchorage. The need for selective weakening of the slabs to achieve increased beam rotation was shown, but the observation of the energy dissipation still being dominated by the columns highlights the strong effect of the slab despite weakening. This presents an important challenge to transferring damage to the beams. Ignoring obstacles such as slabs and transverse beams may lead to simplified retrofit designs tested in academic research which are not translatable to real buildings. Overall, considering a realistic beam-column joint geometry to assess FRP retrofitting schemes showed that care needs to be taken when design equations are derived from experiments with simplified specimen geometries.

Further research, including experimental and numerical studies on different retrofit layouts, but also looking at specimens with slab but without transverse beams or without slab but with transverse beams, are needed to study this topic further and allow for more general conclusions.

ACKNOWLEDGMENTS

This research is part of the Challenging RISK project funded by the UK Engineering and Physical Science Research Council - EPSRC (EP/K022377/1). The work developed by the author José Melo was partial financially supported by FCT - Fundação para a Ciência e Tecnologia, Portugal, co-funded by the European Social Fund, namely through the post-doc fellowship, with reference SFRH/BPD/115352/2016 and by Base Funding - UIDB/04708/2020 and Programmatic Funding - UIDP/04708/2020 of the CONSTRUCT - Instituto de I&D em Estruturas e Construções - funded by national funds through the FCT/MCTES (PIDDAC). The authors would like to acknowledge the staff of the Civil Laboratory at the University of Aveiro for the support during the experimental campaign. The CFRP and resin used in the experiments was kindly provided by S&P reinforcement.

Declarations of interest: none

REFERENCES

[1] Fardis MN. Seismic Design, Assessment and Retrofitting of Concrete Buildings: based on EN-Eurocode 8. Springer; 2009.

[2] Pohoryles DA, Melo J, Rossetto T, Varum H, Bisby L. Seismic Retrofit Schemes with FRP for Deficient RC Beam-Column Joints: State-of-the-Art Review. J Compos Constr 2019;23:03119001. https://doi.org/10.1061/(ASCE)CC.1943-5614.0000950.

[3] Koutas LN, Tetta Z, Bournas DA, Triantafillou TC. Strengthening of Concrete Structures with Textile Reinforced Mortars: State-of-the-Art Review. J Compos Constr 2019;23:03118001. https://doi.org/10.1061/(ASCE)CC.1943-5614.0000882.

[4] CEN. BS EN 1998-1:2004 Eurocode 8. Design of structures for earthquake resistance. General rules, seismic actions and rules for buildings 2004.

[5] Yu J, Shang X, Lu Z. Efficiency of Externally Bonded L-Shaped FRP Laminates in Strengthening Reinforced-Concrete Interior Beam-Column Joints. J Compos Constr 2016;20:04015064. https://doi.org/10.1061/(ASCE)CC.1943-5614.0000622.

[6] Kam WY, Quintana Gallo P, Akguzel U, Pampanin S. Influence of slab on the seismic response of sub-standard detailed exterior reinforced concrete beam column joints. Proc. 9th US Natl. 10th Can. Conf. Earthq. Eng. Reach. Bord., Toronto, Canada: 2010.

[7] Cheung P, Paulay T, Park R. New Zealand Tests on Full-Scale Reinforced Concrete Beam-Column-Slab Subassemblages Designed for Earthquake Resistance. Spec Publ 1991;123:1–38.

[8] Pohoryles DA, Melo J, Rossetto T. Numerical modelling of FRP-strengthened RC beam-column joints. Proc. 2015 SECED Conf., Cambridge, UK: 2015.

[9] Kouris LA, Borg RP, Indirli M. The L’Aquila Earthquake, April 6th, 2009: a review of seismic damage mechanisms. Proc. Final Conf. COST Action C26 Urban Habitat Constr. Catastrophic Events, Mazzolani, FM September; 2010, p. 16–8.

[10] Pohoryles DA, Rossetto T, Melo J, Varum H. A combined FRP and selective weakening retrofit for realistic pre-1970's RC structures. Proc 1st Int. Conf. Nat. Hazards Infrastruct., Chania, Greece: 2016.
[11] Gallo PQ, Akguzel U, Pampanin S, Carr AJ, Bonelli P. Shake table tests of non-ductile RC frames retrofitted with GFRP laminates in beam column joints and selective weakening in floor slabs. Proc. 2012 NZSEE Conf., Christchurch, NZ: 2012.
[12] Akguzel U, Pampanin S. Recent Developments in Seismic Strengthening of RC Beam-Column Joints with FRP Materials. Proc. 15th World Conf. Earthq. Eng., Lisbon, Portugal: 2012.
[13] Antonopoulos C, Triantafillou T. Experimental Investigation of FRP-Strengthened RC Beam-Column Joints. J Compos Constr 2003;7:39–49. https://doi.org/10.1061/(ASCE)1090-0268(2003)7:1(39).
[14] fib, editor. fib Bulletin 35 - Retrofitting of concrete structures by externally bonded FRPs, with emphasis on seismic applications. Lausanne: fib; 2006.
[15] El-Amoury T, Ghobarah A. Seismic rehabilitation of beam–column joint using GFRP sheets. Eng Struct 2002;24:1397–407. https://doi.org/10.1016/S0141-0296(02)00081-0.
[16] Ghobarah A, El-Amoury T. Seismic Rehabilitation of Deficient Exterior Concrete Frame Joints. J Compos Constr 2005;9:408–16. https://doi.org/10.1061/(ASCE)1090-0268(2005)9:5(408).
[17] fib, editor. fib Bulletin 90 - Externally applied FRP reinforcement for concrete structures. Lausanne: fib; 2019.
[18] Prota A, Nanni A, Manfredi G, Cosenza E. Selective upgrade of underdesigned reinforced concrete beam-column joints using carbon fiber-reinforced polymers. ACI Struct J 2004;101:699–707. https://doi.org/10.14359/13392.
[19] Akguzel U, Pampanin S. Assessment and Design Procedure for the Seismic Retrofit of Reinforced Concrete Beam-Column Joints using FRP Composite Materials. J Compos Constr 2012;16:21–34. https://doi.org/10.1061/(ASCE)CC.1943-5614.0000242.
[20] Del Vecchio C, Di Ludovico M, Balsamo A, Prota A, Manfredi G, Dolce M. Experimental Investigation of Exterior RC Beam-Column Joints Retrofitted with FRP Systems. J Compos Constr 2014;18. https://doi.org/10.1061/(ASCE)CC.1943-5614.0000459.
[21] ACI Committee 440, American Concrete Institute. ACI 440.2R-17 - Guide for the design and construction of externally bonded FRP systems for strengthening concrete structures. 2017.
[22] Pantelides C, Okahashi Y, Reaveley L. Seismic Rehabilitation of Reinforced Concrete Frame Interior Beam-Column Joints with FRP Composites. J Compos Constr 2008;12:435–45. https://doi.org/10.1061/(ASCE)1090-0268(2008)12:4(435).
[23] Pampanin S, Akguzel U, Attanasi G. Seismic Upgrading of 3-D Exterior R.C. Beam Column Joints Subjected To Bi-Directional Cyclic Loading Using GFP Composites, Patras, Greece: 2007.
[24] Engindeniz M, Kahn LF, Zureick AH. Performance of an RC corner beam-column joint severely damaged under bidirectional loading and rehabilitated with FRP composites. Seism. Strength. Concr. Build. Using FRP Compos., Farmington Hills, MI: American Concrete Institute; 2008, p. 19–36.
[25] Pohoryles DA, Melo J, Rossetto T, D'Ayala D, Varum H. Experimental Comparison of Novel CFRP Retrofit Schemes for Realistic Full-Scale RC Beam–Column Joints. J Compos Constr 2018;22:04018027. https://doi.org/10.1061/(ASCE)CC.1943-5614.0000865.
[26] REBA. Governo D. Regulamento de Estruturas de Betão Armado - Decreto n.º 47723. vol. 119. Lisbon, Portugal: 1967.
[27] CEN. BS EN 1996-1-1:2005 Eurocode 6. Design of masonry structures - Part 1-1: General rules for reinforced and unreinforced masonry structures. London: BSI; 2005.
[28] CEN. BS EN 1998-3:2005 - Eurocode 8. Design of structures for earthquake resistance. Assessment and retrofitting of buildings 2006.
[29] CNR. DT 200.R1/2013 - Guide for the Design and Construction of Externally Bonded FRP Systems for Strengthening Existing Structures - Materials, RC and PC structures, masonry structures 2013.
[30] Pohoryles DA. Realistic FRP Seismic Strengthening Schemes For Interior Reinforced Concrete Beam-Column Joints. PhD. University College London, 2017.
[31] Eslami A, Ronagh H. Experimental Investigation of an Appropriate Anchorage System for Flange-Bonded Carbon Fiber–Reinforced Polymers in Retrofitted RC Beam–Column Joints. J Compos Constr 2014;18:04013056. https://doi.org/10.1061/(ASCE)CC.1943-5614.0000456.
[32] Park YJ, Ang AH, Wen YK. Damage-limiting aseismic design of buildings. Earthq Spectra 1987;3:1–26.

[33] Pohoryles D, Melo J, Rossetto T, Varum H, D'Ayala D. Experimental investigation on the seismic FRP retrofit of full-scale RC beam-column joints. Improv. Seism. Perform. Exist. Build. Struct., San Francisco, California: ASCE; 2015, p. 619–31. https://doi.org/10.1061/9780784479728.051.